NÖRO PSİKİYATRİ ARŞİVİ
ARCHIVES OF NEUROPSYCHIATRY

RESEARCH ARTICLE

Arch Neuropsychiatry 2024;61:39–46
https://doi.org/10.29399/npa.28366

Diffusion Tensor Imaging in Parenchymal Neuro-Behçet's Disease

Tuncay GÜNDÜZ[1], Sadık SERVER[2], Cem İsmail KÜÇÜKALİ[3], Onur ÖZYURT[4], Gülşen AKMAN DEMİR[5], Murat KÜRTÜNCÜ[1]

[1]Department of Neurology, Istanbul Faculty of Medicine, Istanbul University, Istanbul, Turkey
[2]Department of Radiology, Istanbul Florence Nightingale Hospital, Demiroğlu Bilim University, Istanbul, Turkey
[3]Department of Neuroscience, Aziz Sancar Institute of Experimental Medicine, Istanbul University, Istanbul, Turkey
[4]Biomedical Engineering, Boğaziçi University, Istanbul, Turkey
[5]Department of Neurology, Faculty of Medicine, Bezmialem Vakıf University, Istanbul, Turkey

ABSTRACT

Introduction: Parenchymal Neuro-Behçet's disease (p-NBD) usually presents with a characteristic lesion in the mesodiencephalic region. However, there is a lack of information regarding the axonal integrity of normal-appearing white matter in p-NBD. Diffusion tensor imaging (DTI) is based on the properties of diffusivity and anisotropy that indicate the integrity of axons. The primary objective of the study was to compare p-NBD patients to healthy controls using diffusion tensor magnetic resonance imaging (DTI-MRI).

Methods: The study enrolled parenchymal p-NBD patients who maintained stable disease status for 12 months. Healthy controls were chosen from a population with a similar age and gender distribution. Axial DTI was acquired using single-shot echo-planar imaging. Group analyses were carried out using the track-based spatial statistics tool of FMRIB software library (FSL). Correlations between DTI parameters and clinical outcomes were analyzed in the patient group.

Results: We recruited 12 patients with p-NBD and 12 healthy individuals. We found significant fractional anisotropy (FA), mean diffusivity (MD), and radial diffusivity (RD) differences in the superior longitudinal fasciculus, superior corona radiata, anterior corona radiata, body and genu of the corpus callosum, external capsule, and anterior limb of the internal capsule, mainly in the frontal white matter.

Conclusion: Patients with p-NBD exhibit significant DTI alterations in the otherwise normal-appearing frontal association tracts. This study may contribute to a better understanding of the neuropsychological impairment pattern in patients with p-NBD, which is often associated with frontal cognitive networks.

Keywords: cognitive involvement, diffusion tensor imaging, frontal white matter tracts, neuro-Behçet's disease

Cite this article as: Gündüz T, Server S, Küçükali Cİ, Özyurt O, Akman Demir G, Kürtüncü M. Diffusion Tensor Imaging in Parenchymal Neuro-Behçet's Disease. Arch Neuropsychiatry 2024;61:39–46.

INTRODUCTION

Behçet's disease (BD) is a multi-systemic and inflammatory disease with a relapsing-remitting or progressive clinical course. It is mainly seen along the Silk Road from Japan to the Middle East, with a wide range of prevalence (e.g., 20–141/100,000 in Turkey, 0.64/100,000 in the UK) (1). There is still no consensus regarding the disease's general pathophysiology; several experts categorize BD as autoinflammatory, autoimmune, or MHC-1-opathy (spondyloarthropathy) (2–5). In 1937, BD was described as a group of symptoms that included uveitis, oral and genital ulcers. However, over the years, other organs were shown to be affected, including the nervous system (Neuro-Behçet's disease, NBD) (6).

Neuro-Behçet's disease (NBD) most commonly presents with brain parenchymal (60–80%) and vascular involvement (Dural venous sinus thrombosis, 10–20%). In the acute phase, neurological findings may be observed due to brain stem and diencephalic lesions which are typically contrast-enhancing with perilesional vasogenic edema. In the chronic phase, somatic and cognitive neurological dysfunction and atrophy in the regions mentioned above may develop (7). While conventional and volumetric MRI can detect atrophy, another sensitive tool is required to determine the structural integrity of white matter tracts and their relation to neurological deficits in NBD patients.

Highlights

- **Parenchymal neuro-Behçet's disease leads to altered diffusion tensor imaging values.**
- **DTI metrics are mostly affected in NBD patients' normal-appearing frontal white matter.**
- **DTI alterations may explain the executive dysfunction in parenchymal NBD patients.**
- **DTI may be a useful tool for the diagnosis and follow-up in NBD patients.**

Diffusion tensor imaging (DTI) estimates the location, orientation, and anisotropy of the brain's white matter tracts by measuring water diffusion and can assess microstructural changes in the brain. These measures can be calculated by radial diffusivity (perpendicular to the tract), axial diffusivity (parallel to the tract), mean diffusivity (a measure of mean diffusion in each direction), and fractional anisotropy values, which

Correspondence Address: Murat Kürtüncü, İstanbul Üniversitesi, İstanbul Tıp Fakültesi, Nöroloji Anabilim Dalı, Çapa, Fatih, İstanbul, Turkey • **E-mail:** kurtuncum@gmail.com
Received: 26.11.2022, **Accepted:** 10.01.2023, **Available Online Date:** 27.02.2024

measure the total magnitude of directional water movement along the axonal fibers (8–10). Water diffusion through intact axon bundles in the brain leads to a dominant directional flow, namely anisotropic flow. Chronic injury associated with demyelination and axonal loss leads to reduced anisotropy (10). Cognitive decline and disconnection of various cerebral regions have been previously linked to the loss of axonal integrity within white matter tracts (11). Only a few diffusion MRI studies have been conducted in patients with NBD (12,13). They discovered decreased diffusivity in the normal-appearing frontal, temporal, and occipital regions on conventional MRI sequences. Currently, the predictive value of DTI-MRI for somatic and cognitive neurological impairment in NBD patients is unknown. The main objective of this study was to compare the white matter microstructures of patients with NBD and healthy individuals by employing DTI and then to correlate the DTI findings with the neurological disability status.

METHOD

Participants

Stable NBD patients without any comorbid neurological disease, and without any steroid treatment within the last 12 months were included in the study. Healthy controls were selected from a group of individuals with a similar age and gender distribution. The study was approved by the local ethics committee of Istanbul Faculty of Medicine (approval number: 2009/2982-119). To determine the neurological disability at the time of MRI, the modified Rankin score (mRS), expanded disability status scale (EDSS) score (14), and NBD disability score (NBDS) were recorded. The NBDS is a novel scale designed to assess the combined impact of physical and cognitive disability in NBD patients (Table 1). A score of 0 corresponds to a normal neurological examination, and eight to death due to NBD (15,16).

Magnetic Resonance Imaging Data Acquisition

Magnetic resonance imaging was performed using a 3-T scanner (GE Signa HDxt, Milwaukee, USA) with an 8-channel head coil. Axial DTI was acquired using a single-shot echo-planar imaging and an acceleration factor of 2.00 (TR/TE=17000/89.2 ms, 36 slices, slice thickness=3 mm, interslice gap=0.5 mm, matrix=256×256, in-plane resolution=0.875×0.875 mm, NEX=2, number of gradient directions=13, b values=0 and 1000 s/mm^2, scanning time=15 min 01 s). Additionally, a high resolution sagittal T1-weighted 3D gradient-echo sequence (TR/TE=8.41/3.3 ms, 170 slices, slice thickness=1 mm, interslice gap=0 mm, matrix=512×512, NEX=1, in-plane resolution=0.43×0.43 mm, flip angle=12°, scanning time=4 min 26 s) structural images of the entire brain were acquired for anatomical reference.

Tract-Based Spatial Statistics Analysis

Diffusion tensor imaging analyses were carried out using the FMRIB software library (FSL) (17). For each subject, the diffusion-weighted images (DWI) were corrected for head motion and eddy currents using the eddy correct tool of FSL. These DTI parameter maps were created using the corrected DWI data: fractional anisotropy (FA), mean diffusivity (MD), axial diffusivity (AD), and radial diffusivity (RD). Group analyses were carried out using the track-based spatial statistics (TBSS) tool of FSL (18). Each subject's FA map was registered to an FMRIB58-FA standard-space image. A study-specific mean-FA image and WM skeleton in MNI152 standard space was created for further analysis. The DTI parameter maps for each patient were then placed on this skeleton for use in the voxel-wise group analysis. Unpaired t-tests were used to determine differences in DTI parameter maps between NBD patients and the healthy controls. Multiple comparisons were performed using threshold-free cluster enhancement (TFCE) using 5000 permutations. The TFCE images (corrected for multiple comparisons across space) were used to determine statistical significance, with a p-value threshold of 0.05. The correlations between DTI parameters and clinical outcomes in the patient group were investigated using permutation-based linear correlation analysis. The EDSS, mRS, and NBDS were included as factors of interest in the design matrices.

RESULTS

We enrolled 12 patients (6 males and 6 females) with parenchymal neuro-Behçet's disease and 12 healthy individuals into our study. The demographic and clinical features of the participants are depicted in Table 2. During the clinical course of the disease, all patients received azathioprine, three patients received intravenous cyclophosphamide, and one patient received infliximab. Patients had mild to moderate neurological disability at the time of the MRI acquisition (mRS range: 1–3, EDSS range: 1.5–4.0, NBDS range: 0–8).

Retrospective evaluation of all conventional MRIs performed at the time of NBD relapses revealed that the lesions were located in the bulbus in three patients, pons in four patients, mesencephalon in ten patients,

Table 1. Neuro-Behçet's disease disability score is calculated by the sum of functional scores in motor and cognitive domains. Death due to NBD=8 points

Motor status score (MSS)
0: Normal neurological examination
1: Signs only. Findings do not interfere with daily activities. The patient is independent. Fully ambulatory without aid.
2: Mild disability. Findings interfere with daily activities. The patient is independent. Ambulatory without aid or rest more than 100 mt.
3: Patient is dependent. The patient has effective use of his upper extremity. Retains some self-care functions, but is dependent on many daily activities. The patient can walk more than 5 mt. without aid. Able to transfer from wheelchair to bed independently.
4: Essentially restricted to wheelchair or bed. The patient is dependent on a caregiver for most of the daily activities. Not able to walk 5 mt. independently. Confined to bed for more than half of the day.
X: Other organ involvement (e.g., ophthalmic, orthopedic, vascular, etc.) that interferes with assessment.
Cognitive status score (CSS)
0: Normal
1: Patient complains of forgetfulness. The patient is worried about memory problems that do not interfere with daily activities.
2: Cognitive disability that interferes with many of the daily activities or disturbed social relationships or patient is not able to work or there is pseudobulbar affect.
3: Incapable of doing the majority, if not all, everyday activities or fully dependent because of cognitive impairment or cognitive disturbance fulfilling criteria for dementia.

Neuro-Behçet's Disability Score (NBDS)=MSS + CSS

Table 2. Demographic and clinical profile of the study participants

	NBD patients (n=12)	Healthy volunteers (n=12)	p
Age	39.6 (±6.1)	38.2 (±6.4)	0.61
Gender	6 M. 6 F	6 M. 6 F	0.65
Age at BD onset	27.5 (±4.8)		
Age at NBD onset	32.4 (±5.8)		
Time between last relapse and DTI-MRI (years, mean)	5.1 (±3.8)		
Total number of relapses until DTI-MRI (mean)	2 (±0.9)		
At the time of DTI-MRI			
EDSS (mean)	2.9 (±1.0)		
Modified Rankin Score (mean)	2 (±0.9)		
NBDS (mean)	3 (±1.4)		

The standard deviations are indicated in brackets. BD: Behçet's disease; EDSS: expanded disability status scale; F: Female; M: Male; NBD: neuro-Behçet's disease; NBDS: neuro-Behçet's disease disability score; DTI-MRI: Diffusion tensor magnetic resonance imaging.

diencephalon in six patients, and the cerebellum in one patient. Nine patients had lesions in more than one anatomical region (Figure 1).

The TBSS analysis of the NBD patients showed a significant FA decrease in the right superior longitudinal fasciculus, superior corona radiata, anterior corona radiata, body and genu of corpus callosum, external capsule, and left anterior corona radiata (Figure 2, Table 3).

Additionally, a significant MD increase was detected in the body and genu of the corpus callosum, bilateral anterior corona radiata, superior corona radiata, right anterior limb of the internal capsule, external capsule, and superior longitudinal fasciculus (Figure 2, Table 4).

Neuro-Behçet's disease patients also showed increased RD in the body and genu of the corpus callosum, bilateral anterior corona radiata, superior corona radiata, right external capsule, anterior limb of the internal capsule, and superior longitudinal fasciculus (Figure 2, Table 5). No statistically significant difference was observed in the AD values between the patients and the control subjects (P>0.05). Additionally, we found significant correlations between DTI metrics (FA, RD) and clinical disability score mRS across various regions (Table 6).

DISCUSSION

Neurological involvement in BD is a major cause of morbidity. Almost 80% of the patients with NBD have parenchymal involvement (p-NBD). Half of the patients with p-NBD have lesions in the mesodiencephalic junction extending along the anterior craniocaudal tracts that present as a "cascade sign" in coronal MR T2-weighted or FLAIR images (19). The thalamus and pons are the second most afflicted areas, with just 8% of cases having telencephalic lesions (20). Conventional MRI findings and different contrast enhancement patterns of active and chronic parenchymal NBD lesions have been extensively reported in various studies.

Other imaging modalities, such as magnetization transfer ratio (MTR) and diffusion-weighted imaging, have recently been reported in NBD patients, shedding light on the pathophysiology of the disease. In one of them, Anik et al. compared the MTR of NBD patients and healthy controls. Among the normal-appearing ten anatomical regions, they found a statistically significant MTR increase only in the thalamus (21). A further study found higher apparent diffusion coefficient (ADC) values in both acute and chronic p-NBD lesions, indicating nonischemic tissue damage (22).

Another diffusion-weighted imaging technique, DTI, reveals information about disorganized or disconnected white matter tracts. As a result, it is a potential tool for studying microstructural alterations in neuropathology and treatment. White matter tracts running in parallel in bundles of axonal fibers are the targets of the DTI. The principle of the DTI relies on the fact that the diffusion in the parallel fibers is faster than in the perpendicular fibers. Based on the direction of the fastest diffusion, color-coded maps that represent the orientation of the white matter tracts are generated using FA, MD, and RD. The key output value of DTI is FA, which reflects the displacement of water molecules along axonal fibers. In other words, it is a measure of water molecule diffusion asymmetry inside a voxel. Fractional anisotropy decreases in response to disrupted longitudinal diffusivity, excessive perpendicular diffusivity, or a combination of these two factors. As a result, FA and MD demonstrate changes in diffusion barriers; increased axial diffusivity is linked to axonal degeneration, whereas increased RD is related to demyelination (23). In patients with chronic inflammatory demyelinating polyneuropathy, Kronlage et al. found that FA and RD were significantly related to electrophysiological indicators of demyelination (24). Furthermore, FA is linked to gray matter astrogliosis, whereas MD is associated with enhanced cellularity (10). In another study, FA was shown to have a strong correlation with the axonal integrity in an animal model traumatic brain injury (25).

In our study, we employed DTI metrics as a surrogate tool to detect tract integrity in the normal-appearing white matter in patients with p-NBD. We identified low FA, high MD, and RD values across various regions of the brain. Interestingly, tracts of the normal-appearing frontal white matter were affected substantially in the DTI parameter maps. This novel finding might assist in understanding the pattern of neuropsychological impairment exhibited in patients with p-NBD, which typically involves frontal networks.

There is a limited number of studies that utilize DTI in patients with BD, showing abnormalities in the normal-appearing white matter tracts. In one of them, Aykac et al. found lower FA values in the posterior limb of the internal capsule and cerebral peduncles bilaterally in patients with BD and NBD, suggesting asymptomatic involvement of the corticospinal tracts (26). In another study, Atasoy et al. investigated subclinical cerebral involvement in BD patients using DTI and correlated ADC, FA, MD, and RD

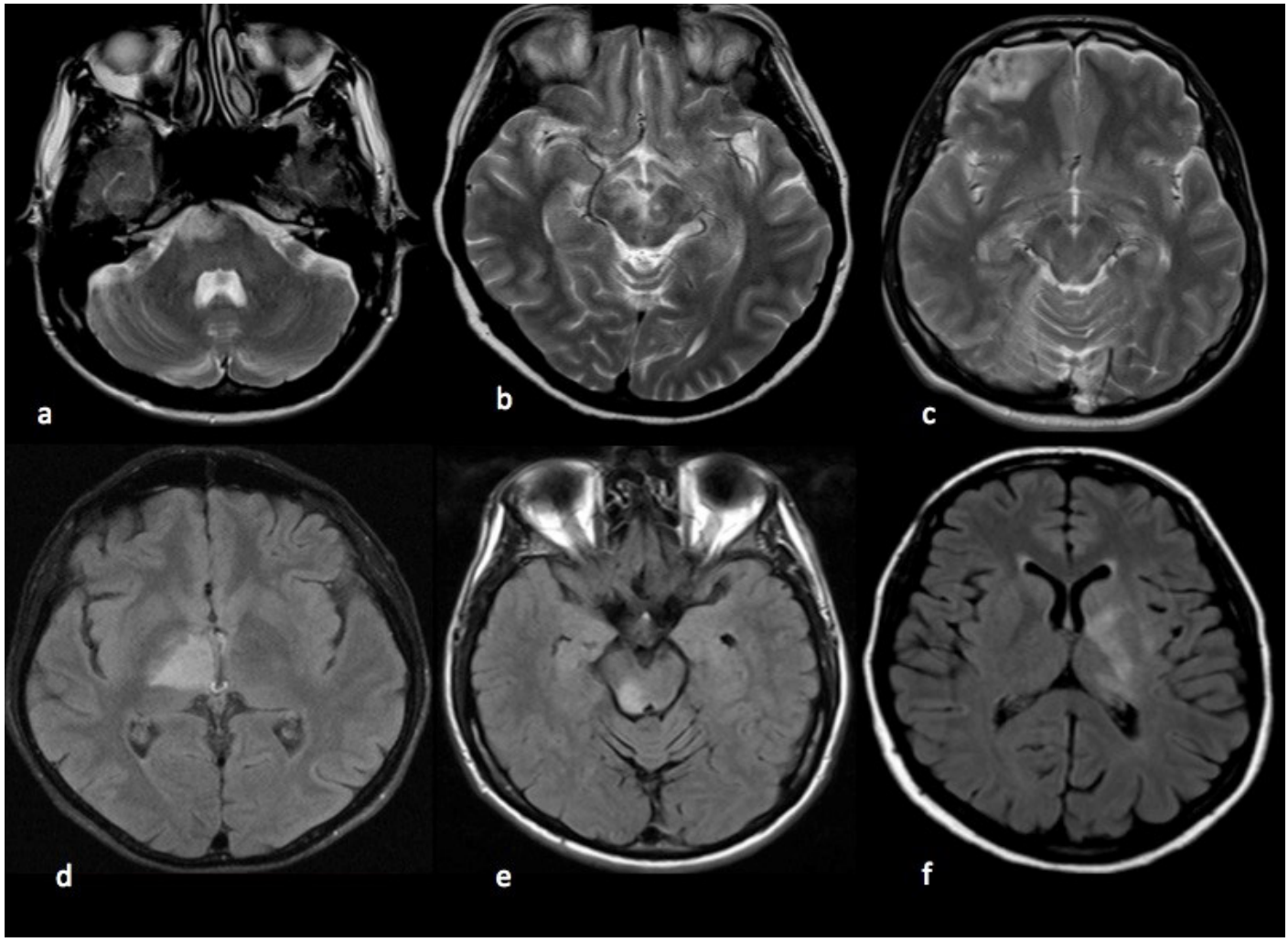

Figure 1. Parenchymal NBD lesions of six different patients during the acute attack. T2 lesions in anterior pons **(a),** right anteromedial mesencephalon **(b),** and right anterior frontal lobe **(c).** T2 FLAIR lesions in right thalamus **(d),** right posterolateral mesencephalon, **(e)** and left thalamus including capsula interna **(f)**

values in 19 cerebral regions with the disease duration and neurocognitive tests. In BD patients, they found lower FA values in the cingulum and splenium and higher RD values in the superior longitudinal fasciculus and splenium compared to controls. They also reported a correlation between the FA values of the cingulum, genu of the corpus callosum, and the posterior limb of the internal capsule with the duration of the disease. Moreover, they discovered a relationship between MD values of the parieto-occipital white matter and the selective reminding test (27).

Neuropsychological deficits are reported in 30–100% of NBD patients. Presenting predominantly as frontal executive dysfunction and memory impairment, patients may also complain of personality changes and other psychiatric disorders, including kleptomania (28). Frontal executive dysfunction such as deterioration in response inhibition and perseverations with variable severity is frequent (29). Patients may also complain of apathy, depression, pseudobulbar affect, and disinhibition affecting many aspects of their daily lives. Interestingly, cognitive dysfunction in memory and executive domains is also observed in 45% of BD patients without neurological involvement, suggesting subclinical involvement of the frontal networks in BD (30,31).

Supporting our observations, frontal abnormalities in NBD have been identified in studies utilizing several imaging modalities. For example, Park-Matsumoto et al. found bilateral frontal hypoperfusion on single-photon emission tomography (SPECT) in a p-NBD patient with bilateral thalamic lesions who presented with mutism (32). Additionally, García-Burillo et al. found abnormal HMPAO brain SPECT in BD patients with neuropsychiatric symptoms and even in asymptomatic patients, indicating dysfunctional perfusion or local metabolic disturbance as early subclinical central nervous system involvement. Interestingly, they also reported that the most common abnormality occurred in the frontal lobes in 48% of cases (33).

In p-NBD, the underlying pathophysiology of the frontal dysfunction is obscure because direct involvement of the frontal cortex is exceedingly rare in p-NBD, which predominantly affects the mesodiencephalic region. The interruption of the cerebello-thalamo-cerebro-cortical circuits (CTCC), which contains telencephalic projections from the cerebellum via relay networks in the brainstem and thalamus, may be the reason for frontal dysfunction in NBD. Another example, the cerebellar affective syndrome, is a distinctive condition caused by CTCC disruption. Executive functions, language processing, spatial cognition, and emotional dysregulation are observed in CTCC that is comparable with the frontal executive dysfunction seen in NBD patients (28).

Our study has two limitations. First, we do not have any longitudinal data that may reveal the onset of the DTI findings. Second, the patients lack a comprehensive neuropsychological assessment. As a result, we were not able to correlate the DTI findings with the neuropsychological impairment.

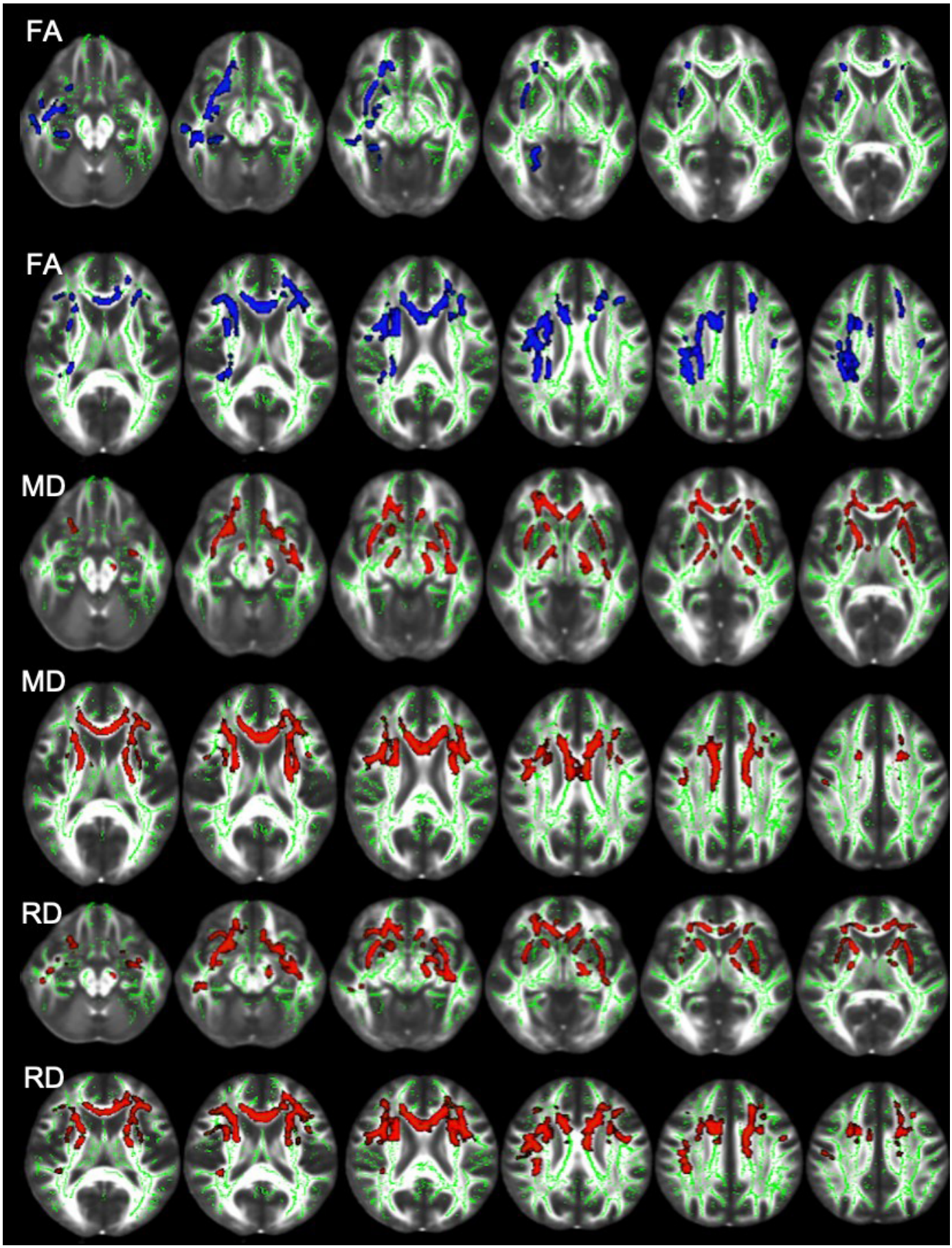

Figure 2. Differences in FA, MD, and RA between controls and neuro-Behçet's disease patients. Blue regions in FA images and red regions in MD and RD images indicate lower FA, and higher MD and RD for the patient group ($p<0.05$). Fractional anisotropy skeleton (green) was overlaid on the mean FA volume (FMRIB58) provided by FSL (FA: fractional anisotropy; MD: mean diffusivity; RA: radial diffusivity).

Table 3. Neuroanatomic regions with significantly decreased fractional anisotropy in neuro-Behçet's patients compared with the control group

Anatomic regions	FA cluster size (mm^3)	FA p-value
R-SLF	667	0.045
R-SCR	509	0.045
R-ACR	439	0.04
BCC-B	432	0.037
CC-G	410	0.038
R-EC	405	0.038
L-ACR	192	0.038
R-C	82	0.049
R-SFOF	57	0.034
R-UF	38	0.043
R-ALIC	20	0.036
L-SCR	10	0.04
L-C	7	0.039
R-PLIC	6	0.049
L-SLF	6	0.049

CC-B: corpus callosum body; CC-G: corpus callosum genu; L-ACR: left anterior corona radiata; L-SCR: left superior corona radiata; L-SLF: left superior longitudinal fasciculus; R-ACR: right anterior corona radiata; R-ALIC: right anterior limb of the internal capsule; R-C: right cingulum; R-C: right cingulum; R-EC: right capsula externa; R-PLIC: right posterior limb of the internal capsule; R-SCR: right superior corona radiata; R-SFOF: right superior fronto-occipital fasciculus; R-SLF: right superior longitudinal fasciculus; R-UF: right uncinate fasciculus.

Table 4. Neuroanatomical regions with significantly increased mean diffusivity in NBD patients compared with the control group

Anatomical regions	MD cluster size (mm^3)	MD p-value
CC-B	1170	0.038
CC-G	902	0.036
R-ACR	677	0.036
L– ACR	500	0.038
R-ALIC	388	0.049
R-EC	353	0.049
L-SCR	292	0.038
R-SCR	201	0.049
R-SLF	190	0.049
R-PLIC	125	0.041
L-SLF	61	0.044
R-SFOF	55	0.036
R-UF	33	0.034
R-C	23	0.049
L-C	11	0.036

CC-B: corpus callosum body; CC-G: corpus callosum genu; L-ACR: anterior corona radiata; L-C: left cingulum; L-SCR: left superior corona radiata; L-SLF: left superior longitudinal fasciculus; R-ACR: right anterior corona radiata; R-ALIC: right anterior limb of the internal capsule; R-C: right cingulum; R-EC: right capsula externa; R-PLIC: right posterior limb of the internal capsule; R-SCR: right superior corona radiata; R-SFOF: right superior fronto-occipital fasciculus; R-SLF: right superior longitudinal fasciculus; R-UF: right uncinate fasciculus.

Using DTI, we demonstrated FA, RD, and MD alterations in patients with p-NBD compared to healthy controls, particularly in the frontal white matter tracts. This result corroborates earlier studies implying a distinctive cognitive deficit in p-NBD, mainly as frontal executive dysfunction. Emerging evidence shows that the brain pathology in NBD precedes clinical symptoms. Pre-symptomatic alterations must be recognized in order to allow for intervention as early as possible. Because it is non-invasive and easy to repeat, MRI is the most suitable way for revealing early changes in the brain. Future research should focus on delving deeper into the correlations between DTI metrics and cognitive function to evaluate whether DTI has the potential to monitor the clinical progression of NBD.

Ethics Committee Approval: The study was approved by the local ethics committee of Istanbul Faculty of Medicine (approval number: 2009/2982-119).

Informed Consent: All study participants provided written informed consent.

Peer-review: Externally peer-reviewed.

Table 5. Neuroanatomical regions with significantly increased radial diffusivity in NBD patients compared with the control group

Anatomical regions	RD-Cluster size (mm^3)	RD-p-value
CC-B	871	0.045
CC-G	847	0.029
R-ACR	585	0.034
L-ACR	507	0.029
R-EC	457	0.045
R-SCR	316	0.04
R-ALIC	300	0.031
L-SCR	260	0.045
R-SLF	250	0.034
L-SLF	92	0.031
R-C	81	0.045
R-PLIC	62	0.045
R-SFOF	61	0.029
R-UF	38	0.029
L-C	21	0.03

CC-B: corpus callosum body; CC-G: corpus callosum genu; L-ACR: anterior corona radiata; L-C: left cingulum; L-SCR: left superior corona radiata; L-SLF: left superior longitudinal fasciculus; R-ACR: right anterior corona radiata; R-ALIC: right anterior limb of the internal capsule; R-C: right cingulum; R-EC: right capsula externa; R-PLIC: right posterior limb of the internal capsule; R-SCR: right superior corona radiata; R-SFOF: right superior fronto-occipital fasciculus; R-SLF: right superior longitudinal fasciculus; R-UF: right uncinate fasciculus.

Table 6. Neuroanatomical regions exhibiting a positive correlation on the FA map and a negative correlation on the RD map with MRS scores

	FA-MRS (positive correlation)		RD-MRS (negative correlation)	
Anatomical regions	Cluster size (mm^3)	p-value	Cluster size (mm^3)	p-value
CC-B	871.0	0.030	534.0	0.036
CC-S	461.0	0.019	172.0	0.036
L-ALIC	48.0	0.039	–	NS
R-RLIC	56.0	0.020	–	NS
L-RLIC	226.0	0.044	20.0	0.049
L-ACR	89.0	0.049	–	NS
R-SCR	138.0	0.044	–	NS
L-SCR	229.0	0.041	42.0	0.049
R-PCR	442.0	0.024	155.0	0.049
L-PCR	483.0	0.019	383.0	0.035
R-PTR	143.0	0.021	8.0	0.048
L-PTR	449.0	0.013	217.0	0.030
L-SS	39.0	0.044	4.0	0.049
L-EC	64.0	0.039	–	NS
L-C	8.0	0.021	–	NS
R-SLF	338.0	0.044	–	NS
L-SLF	328.0	0.044	213.0	0.041
L-SFOF	43.0	0.044	–	NS
R-T	15.0	0.018	–	NS

CC-B: corpus callosum body; CC-S: corpus callosum splenium; L-ACR: left anterior corona radiata; L-ALIC: left anterior limb of the internal capsule; L-C: left cingulum (cingulate gyrus); L-EC: left capsula externa; L-PCR: left posterior corona radiata; L-PTR: left posterior thalamic radiation (include optic radiation); L-RLIC: left retrolenticular part of the internal capsule; L-SCR: left superior corona radiata; L-SFOF: left superior fronto-occipital fasciculus (could be a part of anterior internal capsule); L-SLF: left superior longitudinal fasciculus; L-SS: Sagittal stratum (include inferior longitudinal fasciculus and inferior fronto-occipital fasciculus); NS: not significant; R-PCR: right posterior corona radiata; R-PTR: right posterior thalamic radiation (include optic radiation); R-RLIC: right retrolenticular part of internal capsule; R-SCR: right superior corona radiata; R-SLF: right superior longitudinal fasciculus; R-T: right tapetum.

Author Contributions: Concept- TG, SS, MK; Design- TG, SS; Supervision- GAD, MK; Resource- CİK; Materials- TG, SS; Data Collection and/or Processing- TG, OÖ; Analysis and/or Interpretation- TG, OÖ, MK; Literature Search- OÖ, TG; Writing- TG, SS, GAD, MK; Critical Reviews- GAD, MK.

TG and SS contributed equally to the first authorship

Conflict of Interest: O. Ö. received a grant from Nöroimmünoloji Derneği, Türkiye for technical analysis of DTI images. Other authors declare no competing interests.

Financial Disclosure: This work was supported by grants from the Neuroimmunology Society (NIMDER), Turkey. This grant has no influences on the writing of the manuscript or the decision to submit it for publication.

REFERENCES

1. Yurdakul S, Yazici H. Behcet's syndrome. Best Pract Res Clin Rheumatol. 2008;22(5):793–809. [Crossref]
2. Gul A. Pathogenesis of Behcet's disease: autoinflammatory features and beyond. Semin Immunopathol. 2015;37(4):413–418. [Crossref]
3. Hatemi G, Karatemiz G, Yazici H. Behcet's disease: an MHC-I-opathy? Clin Exp Rheumatol. 2017;35 Suppl 104(2):5.
4. Leccese P, Alpsoy E. Behcet's disease: An overview of etiopathogenesis. Front Immunol. 2019;10:1067. [Crossref]
5. McGonagle D, Aydin SZ, Gul A, Mahr A, Direskeneli H. 'MHC-I-opathy'-unified concept for spondyloarthritis and Behcet disease. Nat Rev Rheumatol. 2015;11(12):731–740. [Crossref]
6. Behçet H. Über rezidivierende, aphthöse, durch ein Virus verursachte Geschwüre am Mund, am Auge und an den Genitalien. Dermatol Wschr. 1937;105(36):1152–1157.
7. Gunduz T, Kurtuncu M, Matur Z, Tuzun E, Limon U, Tanyildiz B, et al. Laboratory and clinical correlates of brain atrophy in neuro-Behcet's disease. J Neurol Sci. 2020;414:116831. [Crossref]
8. Song SK, Sun SW, Ju WK, Lin SJ, Cross AH, Neufeld AH. Diffusion tensor imaging detects and differentiates axon and myelin degeneration in mouse optic nerve after retinal ischemia. Neuroimage. 2003;20(3):1714–1722. [Crossref]
9. Song SK, Sun SW, Ramsbottom MJ, Chang C, Russell J, Cross AH. Dysmyelination revealed through MRI as increased radial (but unchanged axial) diffusion of water. Neuroimage. 2002;17(3):1429–1436. [Crossref]
10. Winklewski PJ, Sabisz A, Naumczyk P, Jodzio K, Szurowska E, Szarmach A. Understanding the physiopathology behind axial and radial diffusivity changes -what do we know? Front Neurol. 2018;9:92. [Crossref]
11. O'Sullivan M, Jones DK, Summers PE, Morris RG, Williams SC, Markus HS. Evidence for cortical "disconnection" as a mechanism of age-related cognitive decline. Neurology. 2001;57(4):632–638. [Crossref]
12. Baysal T, Dogan M, Karlidag R, Ozisik HI, Baysal O, Bulut T, et al. Diffusion-weighted imaging in chronic Behcet patients with and without neurological findings. Neuroradiology. 2005;47(6):431–437. [Crossref]
13. Kunimatsu A, Abe O, Aoki S, Hayashi N, Okubo T, Masumoto T, et al. Neuro-Behcet's disease: analysis of apparent diffusion coefficients. Neuroradiology. 2003;45(8):524–527. [Crossref]
14. Siva A, Kantarci OH, Saip S, Altintas A, Hamuryudan V, Islak C, et al. Behcet's disease: diagnostic and prognostic aspects of neurological involvement. J Neurol. 2001;248(2):95–103. [Crossref]
15. Emekli AS, Ersozlu E, Emekli MA, Gunduz T, Kurtuncu M. Lesion distribution pattern of parenchymal neuro-Behcet's disease using probability mapping. Mult Scler Relat Disord. 2022;58:103457. [Crossref]
16. Kurtuncu M, Aydin BN, Gunduz T, Ala S, Akman-Demir G. Neuro-Behcet's disease: Analysis of 430 patients. J Neurol Sci. 2017;381(S):121–122. [Crossref]
17. Smith SM, Jenkinson M, Woolrich MW, Beckmann CF, Behrens TE, Johansen-Berg H, et al. Advances in functional and structural MR image analysis and implementation as FSL. Neuroimage. 2004;23 Suppl 1:S208-219. [Crossref]
18. Smith SM, Jenkinson M, Johansen-Berg H, Rueckert D, Nichols TE, Mackay CE, et al. Tract-based spatial statistics: voxelwise analysis of multi-subject diffusion data. Neuroimage. 2006;31(4):1487–1505. [Crossref]
19. Kürtüncü M, Tüzün E, Akman-Demir G. Behçet's disease and nervous system involvement. Curr Treat Options Neurol. 2016;18(5):19. [Crossref]
20. Kocer N, Islak C, Siva A, Saip S, Akman C, Kantarci O, et al. CNS involvement in neuro-Behcet syndrome: an MR study. AJNR. 1999;20(6):1015–1024.
21. Anik Y, Kural Z, Demirci A, Akansel G, Aksu S, Vural M. Magnetization transfer ratio in neuro-Behcet disease. Neuroradiology. 2005;47(2):108–113. [Crossref]
22. Alis D, Alis C, Tutuncu M, Kocer N, Islak C, Kizilkilic O. Apparent diffusion coefficient characteristics of parenchymal neuro-Behcet's disease. Int J Rheum Dis. 2019;22(8):1452–1458. [Crossref]
23. Alves GS, Oertel Knochel V, Knochel C, Carvalho AF, Pantel J, Engelhardt E, et al. Integrating retrogenesis theory to Alzheimer's disease pathology: insight from DTI-TBSS investigation of the white matter microstructural integrity. Biomed Res Int. 2015;2015:291658. [Crossref]
24. Kronlage M, Pitarokoili K, Schwarz D, Godel T, Heiland S, Yoon MS, et al. Diffusion tensor imaging in chronic inflammatory demyelinating polyneuropathy: diagnostic accuracy and correlation with electrophysiology. Invest Radiol. 2017;52(11):701–707. [Crossref]
25. Tu TW, Williams RA, Lescher JD, Jikaria N, Turtzo LC, Frank JA. Radiological-pathological correlation of diffusion tensor and magnetization transfer imaging in a closed head traumatic brain injury model. Ann Neurol. 2016;79(6):907–920. [Crossref]
26. Aykac SC, Gokcay F, Calli C. What is the role of diffusion tensor imaging (DTI) in detecting subclinical pyramidal tract dysfunction in Behcet's and neuro-Behcet's cases? Neurol Sci. 2019;40(4):753–758. [Crossref]
27. Atasoy B, Toprak H, Su Kucuk O, Selvitop R, Yaman A, Gursoy E, et al. Relationship of diffusion tensor imaging parameters with neurocognitive dysfunction in patients with Behcet's disease. Acta Neurol Belg. 2022;122(5):1177–1186. [Crossref]
28. Gündüz T, Ertekin E. Neuropsychiatric symptoms in Neuro-Behçet's disease. In: Tüzün E, Kürtüncü M, editors. Neuro-Behçet's Disease. Springer Verlag; 2021. p. 107-121. [Crossref]
29. Oktem-Tanor O, Baykan-Kurt B, Gurvit IH, Akman-Demir G, Serdaroglu P. Neuropsychological follow-up of 12 patients with neuro-Behcet disease. J Neurol. 1999;246(2):113–119. [Crossref]
30. Altunkaynak Y, Usta S, Ertem DH, Koksal A, Dirican AC, Baybas S. Cognitive functioning and silent neurological manifestations in Behcet's disease with ocular involvement. Noro Psikiyatr Ars. 2019;56(3):173–177.
31. Monastero R, Camarda C, Pipia C, Lopez G, Camarda LK, Baiamonte V, et al. Cognitive impairment in Behcet's disease patients without overt neurological involvement. J Neurol Sci. 2004;220(1-2):99–104. [Crossref]
32. Park-Matsumoto YC, Ogawa K, Tazawa T, Ishiai S, Tei H, Yuasa T. Mutism developing after bilateral thalamo-capsular lesions by neuro-Behcet disease. Acta Neurol Scand. 1995;91(4):297–301. [Crossref]
33. Garcia-Burillo A, Castell J, Fraile M, Jacas C, Vilardell M, Ortega D, et al. Technetium-99m-HMPAO brain SPECT in Behcet's disease. J Nucl Med. 1998;39(6):950–954.